

## THE ROLE OF ROP GTPASE SIGNALLING IN PLANT MERISTEM FUNCTION

NKFI-1 K 124828

### Final research report

#### Introduction

Our hypothesis-driven research proposal was based on the central hypothesis that RLK-RopGEF-ROP-RLCK VI\_A kinase signalling receptor complexes operate in shoot as well as root meristem maintenance and/or functioning. The existence of RLK-RopGEF-ROP receptor complexes had already been well accepted in plant biology as was summarized in our review article serving the basis of the proposed research (Feher, 2015). In that review article we proposed that the cytoplasmic RLCK VI\_A kinases we earlier identified as ROP GTPase effectors (Dorjgotov *et al.*, 2009), are also part of the receptor complex. Literature and our own preliminary data also indicated that ROP GTPases or RLCK VI\_A kinases are involved in meristem maintenance and functioning. Therefore we aimed to investigate the following hypothetical scenarios: 1) the shoot meristem-size-controlling CLAVATA1 receptor kinase interacts with and activates RopGEF(s); 2) the BELLRINGER1 transcription factor exerts its effects on meristem functions (phyllotaxis, flower morphogenesis), at least partly, via the regulation of the expression of ROPs and their effector kinases; 3) RopGEF7 activates ROP3 and RLCK VI\_A kinases in the root to regulate auxin gradients and post-embryonic meristem maintenance and function; 4) this function of RopGEF7 is post-translationally controlled by the CRK5 kinase affecting the gravitropic response.

During the implementation of the project, we faced several problems. Neither the commercially available but uncharacterized RopGEF antibodies nor the custom RLCK VI\_A antibody worked on plant extracts (only on purified proteins) hampering the direct identification of protein complexes. We realized that the production of transgenic plants expressing tagged-protein versions is too lengthy, especially as we had to stop the experimentation for a considerable time due to the COVID situation. Moreover, due to the forced reorganisation of the institutional network of the Hungarian Academy of Sciences we lost the expertise required to carry out the experiments in a reliable time (our expert Ildiko Valkai left our group and the academic research field due to uncertainties caused by the reorganisation). By that time, the available co-immunoprecipitation, two-hybrid and kinase assay experiments indicated that the existence of the hypothesized protein-protein interactions (e.g., CLAVATA-RopGEF; RopGEF-RLCK VIA2) is unlikely. Therefore, we focused our research efforts to those fields that were more promising to result in original research data and publications even if they were only marginally related to our original working hypothesis. Due to these efforts, we could establish the role of the RLCK VI\_A2 kinase in plant growth, the key role of the CRK5 kinase in the control of auxin transport in embryos and meristems, the link between nitric oxide and ROP GTPase signaling affecting root meristem functioning. We also demonstrated the upstream regulation of ROP GTPases by Calcium Dependent Protein Kinases (CDPKs). Beside these already published results, we identified a number of potential RLCK VI\_A interactors/substrates that serve as the basis for further publications in the near future. Detailed results of the investigations are briefly summarized below.

## Results

### **Hypothesis 1: The shoot meristem-size-controlling CLAVATA1 receptor kinase interacts with and activates RopGEFs.**

This hypothesis was based on a publication (Trotochaud *et al.*, 1999) claiming the presence of putative ROP GTPase in the CLAVATA1 receptor complex.

We asked and obtained (with considerable delay) the CLV1prCLV1GFP in c1-11; CLV1prCLV1GFP in c1-11xc3-2 seeds from Dr. Zachary L. Nimchuk (USA). In these plant lines the CLV1 receptor kinase is expressed under the control of its own promoter in fusion with the Green Fluorescent Protein (GFP) and due to the host genotype, it is more stable and mostly membrane attached where it could more likely interact with RopGEFs. The seeds were propagated and germinated. Shoot meristems of seedlings were collected and used for immunoprecipitation by commercial anti-GFP antibody. Two independent experiments were made. Protein sequencing (MALDI) identified tens of proteins that were represented by at least 4 peptides in the precipitate. In contrast to what was expected, no ROP or RopGEF proteins were among the potential CLV1-interacting ones. However, two receptor-like kinases (FER, TMK4) that are known to interact with RopGEFs could be found in the list, although with low representing peptide numbers. Furthermore, the most likely CLV1 interactors were various plasma membrane (PM) ATPases. CLV1-FER or CLV1-TMK4 receptor kinase heterodimerisation and CLV1-mediated PM ATPase phosphorylation are unprecedented. One could hypothesize that CLV1 may indirectly control ROP signalling via FER/TMK4 kinases and may regulate cell elongation in the meristem via directly controlling PM ATPase activity. To test the hypotheses the corresponding cDNAs were isolated. CLV1, FER, and TMK4 full length, extracellular and cytoplasmic domains were cloned into yeast two-hybrid expression vectors to verify interaction. These tests indicated no interaction. To exclude the possibility that it was due to the non-host yeast system or wrong folding of truncated proteins, we cloned the full-length kinases pairwise into the pDOE11 vector allowing bimolecular fluorescence complementation to take place if the kinases interact in plant cells. We could establish that the receptor kinases did not show interaction in this system either. Further, the kinase domain of CLV1 and one of the the PM ATPase proteins (AHA3) was cloned into bacterial expression vectors and proteins were produced for kinase assay. In the in vitro assay, no phosphorylation of the ATPase in the presence of the CLV1 kinase was detected. Due to the extent of negative results, we gave up this line of research at least temporarily.

It is to be mentioned here that just after the start of the project, the Hungarian Institute of Isotopes Co. Ltd. stopped commercializing radioactive isotopes in Hungary. We previously successfully used P32-gamma-ATP for very sensitive kinase assays serving the basis of several publications (DORJGOTOV *et al.*, 2009; Huesmann *et al.*, 2012; Reiner *et al.*, 2014; Lajkó *et al.*, 2018; Feher *et al.*, 2021). Since we could not afford importing radioactive isotopes from Germany, we attempted adapting various non-radioactive assay kits and formats. Still, we are struggling to find an affordable, simple, and reproducible in vitro kinase assay for our lab. This prevented us e.g., from publishing the identification of potential RLCK VI\_A2 substrates via yeast-2-hybrid and phosphoproteomic approaches (see later).





Figure 2. Example result of testing CLV1-FER interaction by BiFC in onion epidermal cells. Upper left image shows the fluorescence of the independent Blue Fluorescent Protein (BFP) marker validating the success of transfection. The same cell is expected to transiently express both proteins fused to the N- and C-terminal parts of VENUS YFP, respectively. The below image demonstrates that the signal of the YFP protein is missing indicating that it was not reconstituted as there was no CLV1-FER interaction. Upper right image is the bright field image of the same region.

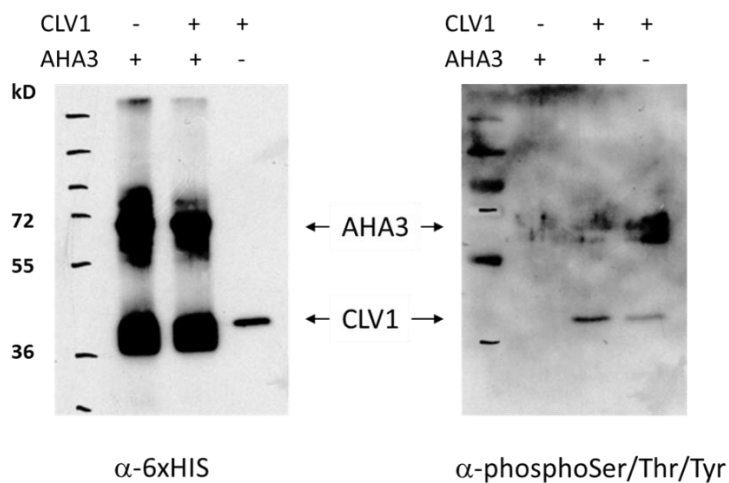


Figure 3. In vitro kinase assay using the purified AHA3 ATPase and the kinase domain of CLV1. The expected size of the ATPase and the CLV1 kinase domain are indicated (the ATPase either co-purifies with a lower MW -app. 38 kD – protein or is cleaved during purification). The autophosphorylation of CLV1 indicates appropriate reaction conditions, which however, did not result in convincing AHA3 phosphorylation.

**Hypothesis 2: The BELLRINGER transcription factor exerts its effects on meristem functions (phyllotaxis, flower morphogenesis), at least partly, via the regulation of the expression of ROPs and their effector kinases.**

This hypothesis was based on the fact that most ROP as well as RLCK VI\_A genes have BLR1-binding sites in their promoters and the BLR and RLCK VI\_A2 loss-of-function resulted in similar phyllotactic aberrations. To support the potential links between the BLR1 transcription factor and the RLCK VI\_A kinase we followed several research directions.

In order to validate the BLR-dependent expression of the RLCK VI\_A2 kinase, we isolated its promoter sequence with a short 5' part of the gene having the first intron (-2928 bp from ATG + 516 bp from the genomic region of the At2G18890 gene with the first intron) from an Arabidopsis BAC library. In the final construct (Fig. 4A) the bacterial  $\beta$ -glucuronidase (GUS) enzyme was translationally fused with the first few aminoacids of the RLCK VI\_A2 protein. The construct was introduced into wild-type and *blr* mutant (obtained from NASC; SALK\_098505) Arabidopsis lines using Agrobacterium-mediated transformation. Transgenic lines were selected, selfed and T2-T3 generation plants were used for testing the kinase promoter regulated expression of the *gus* gene in the two genetic backgrounds. We could confirm that the promoter of the RLCK VI\_A2 kinase is under the control of BLR (Fig. 4B). More detailed analysis of the organ/tissue-specific expression of the kinase gene was also carried out (data not shown).

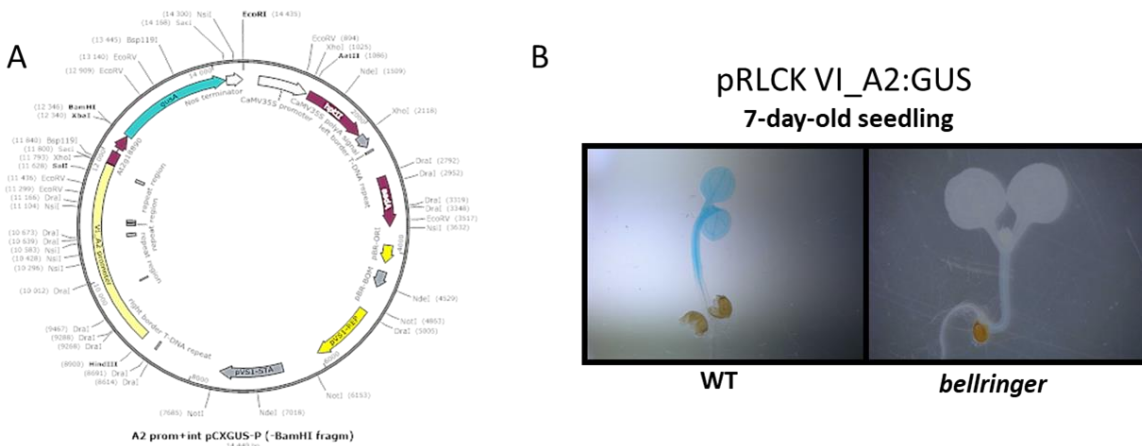


Figure 4 Map of the construct having the bacterial  $\beta$ -glucuronidase (GUS)-coding gene under the control of the RLCK VI\_A2 promoter/intron (A) and the expression of the marker gene in wild type (wt) and *blr* mutant (bellringer) background, respectively (B). The expression in the mutant seedling is barely detectable.

To investigate the functional link between the RLCK\_A2 kinase and the BLR transcription factor, the pK7WGF<sub>2</sub>-VI\_A2 plant vector was prepared containing the *At2G18890* (*rlck vi\_a2*) gene N-terminally fused to a GFP-coding sequence and driven by the CaMV 35S promoter facilitating a high level BLR-independent constitutive expression of the GFP-tagged kinase. Using the floral-dip *Arabidopsis* transformation method we introduced this vector into several *Arabidopsis* plant lines, such as wild type *col-0*, *rlck vi\_a2 KO* (a kinaseVI\_A2 knockout *Arabidopsis* mutant termed also as *gk18*) and the *blr* mutant.

Using *Agrobacterium*-mediated transformation, we generated the RLCK VI<sub>A2</sub> kinase overexpressor *rlck vi\_a2OX col-0* line, the complemented - *rlck vi\_a2CO gk18 Arabidopsis* line, and the *rlck vi\_a2 OX blr* line. Although these plants were selected based on their kanamycin resistance (gained after a successful transformation) and therefore should pose the GFP-fused kinase, we performed anti-GFP Western blots to check whether they do or not express the GFP-fused RLCK VI<sub>A2</sub>. On our surprise not all plants were GFP positive, so for further experiments and for the generation of T2 plants we used only those seedlings, which were able to produce the GFP-fused kinase protein.

These kinase overexpressor lines - *rlck vi\_a2OX col-0*, *rlck vi\_a2OX blr* and *rlck vi\_a2CO gk18* - were used to study the involvement of the VI-A<sub>2</sub> kinase in the phenotypic manifestation of the *blr* mutation. Since *blr* mutants were first described for their abnormal phyllotaxy, two types of phyllotaxy studies were conducted by our group:

- 1.) observation of meristemic phyllotaxy of floral primordia with the aim of scanning electron microscopy (SEM),
- 2.) measurements of divergence angles and internode intervals between two successive inflorescence siliques on mature plants.

**Study of meristemic phyllotaxy.** In general, phyllotaxy can be defined as the arrangement of lateral organs around a central axis. In plants with spiral phyllotaxy (like *Arabidopsis*) the divergence angle between two successive primordia, (measured from the center of the meristem to the middle of two successive organs) is approximately 137.5°. In BELLRINGER mutants of *Arabidopsis* this order is disrupted only in 2 out of 16 mutant plants having significantly reduced divergence angles (range 79.35°-112.13°) indicating abnormal sites of floral meristem initiation (Byrne *et al.*, 2003a).

Phyllotactic measurements were done on apical meristems of untransformed and transformed *Arabidopsis* plants. Measurements showed that the lack of RLCK VI<sub>A2</sub> kinase did not interfere with the shoot meristem phyllotaxy, since buds from *rlck vi\_a2 KO* plants (*gk18*) displayed similar patterns like those collected from *col-0*. Buds of *rlck vi\_a2 KO* plants however, showed a slightly increased meristem surface compared to those of wild type *col0* (Fig. 5). surrounding the meristem and slightly altered phyllotactic angles of growing primordia compared to wild type *col0* (Fig. 5).

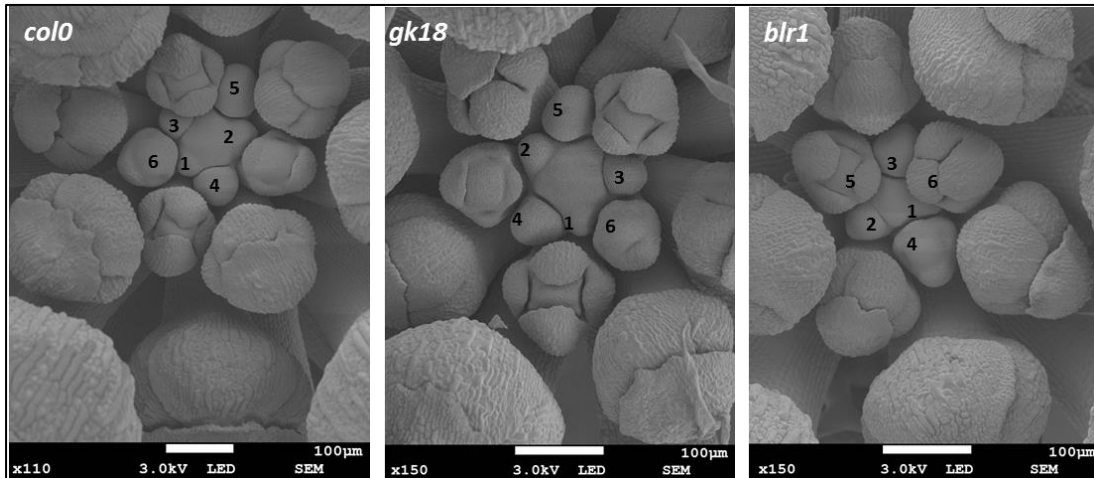


Figure 5. SEM images of shoot meristems of *Arabidopsis* lines used for transformation.

Besides the higher variability in the positioning of two successive primordia within a normal phyllotactic pattern, formation of ectopic primordia was also described in *blr6* mutants (Peaucelle *et al.*, 2011a) (Fig. 6AB).

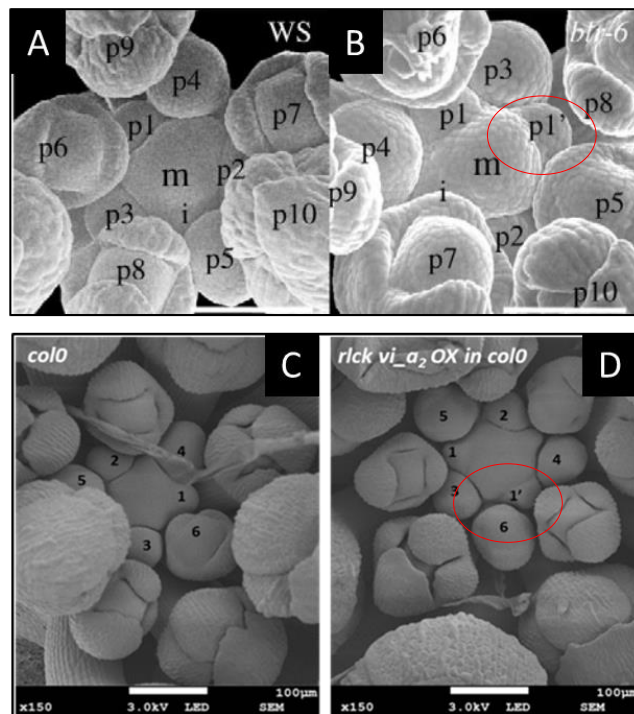


Figure 6. Altered phyllotaxis in the meristem of the *Arabidopsis blr-6* mutant (A,B) and *rlckvi\_a2 OX* transgenic plants (C,D). Ectopic primordia formation in *blr-6* (B) compared with wild type (WS; A) as revealed by scanning electron microscopy (SEM). SEM images representing shoot meristems of buds from *col0* (C) and *rlck\_via2OX* in *col0* (D) lines. Meristem (m), incipient primordia (i) and growing primordia (p1-10) are indicated. Note the ectopic primordium as p1' (encircled). Scale bars: 200µm.

We could not observe this defect in none of the mutant lines presented in Fig. 5 despite the relatively high number of investigated buds. However, the scanning electron microscopy of the kinase VI A<sub>2</sub> overexpressing lines showed that although the ectopic overexpression of RLCK kinase VI\_A<sub>2</sub> did not alter severely the meristemic phyllotaxy of buds, it resulted in slightly increased meristem surface, and we could detect the presence of ectopic primordia in several buds. This could be observed in all genetic backgrounds (*rlck vi\_a2OX col-0*, *rlck vi\_a2CO gk18*, *rlck vi\_a2OX blr*) lines also (Fig. 6), but in the *blr* background the meristem size remained small. Although the formation of ectopic primordia and the increase of shoot meristem surface of *Arabidopsis* lines transformed with the vector expressing the RLCK-VIA<sub>2</sub> kinase under the control of the CaMV 35S promoter could not be observed in all the investigated buds, the expression of the kinase increased the incidence of these phenotypic aberrations.

**Investigation of inflorescence phyllotaxy and internode distances.** In this survey the arrangement of siliques on the main inflorescence stem was studied by measuring the divergence angles and the internode distances between neighbouring organs.

In plants with spiral phyllotaxy the divergence angle between successive siliques is approximately 137.5°, called the „golden angle”. In *col0* wild-type inflorescence apices the average divergence angle is 136.72° (range 121.49°-152.31°) (Byrne *et al.*, 2003b; Peaucelle *et al.*, 2011b). Plants were grown in greenhouse conditions at 12hWL/12hD light cycles and 22°±23°C until stems were fully grown (Fig. 7. and Fig. 8.).



Figure 7. Representative images of stems belonging to wild type *col0*, *rlck\_via2* (*gk18*) and *blr1* knock out plant lines.

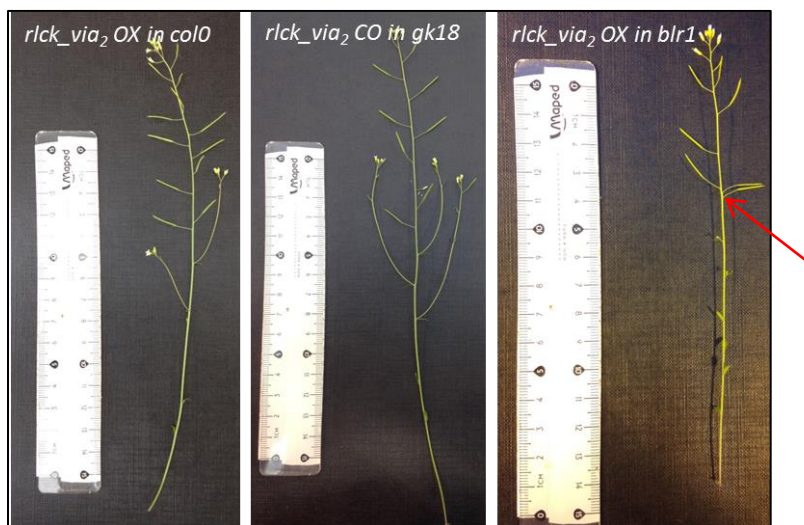


Figure 8. Representative images of stems belonging to wild type *rlck\_via2 OX in col0*, *rlck\_via2 CO in gk18* and *rlck\_via2 OX in blr1* plant lines.

Stems were then cut tightly above rosette leaves; photos of all stems were taken and divergence angles were measured between the insertion points of two successive floral pedicels. Fig. 7. and Fig. 8. shows representative photos of the investigated plant lines. Note the short stem of the *blr*, compared to the *col0* and *gk18*, which correlates with literature data (Byrne *et al.*, 2003a) describing the *blr* mutants as being reduced in stature and having abnormal inflorescence phyllotaxy. The ectopic expression of RLCK-VIA<sub>2</sub> kinase could not complement this phenotype in the *rlck\_via2 OX in blr* line as shown in Fig. 8.

Abnormal phyllotaxy is reflected by the relative displacement of flowers along both the radial and longitudinal axis of the stem. In the radial dimension, flowers can occur both closer together and further apart than in wild type presenting a large range of divergence angles. Inflorescence internode length is also variable so that flowers occur at irregular intervals along the stem (red arrows). The measured divergence angles can be represented as the frequency of occurrence of an angle (%) as a function of degree of divergence between neighbouring siliques. For this, divergence angles between two successive flowers in the meristem were allocated to twelve 30° classes and the percentage of total measurements (*n*) falling into each class is displayed as discussed in (Peaucelle *et al.*, 2011b). In the case of wild type *col0* a Gaussian-like distribution of the divergence angles could be observed, and the average divergence angle was 136,99° (Fig. 9.), being close to the theoretical value of 137,5°.

Since phyllotactic orientation can be either clockwise or anticlockwise, for each individual, the phyllotactic orientation was set to the direction giving the smallest average divergence angle. The kinase knock-out line *gk18* showed a slightly flatter Gaussian distribution of the divergence angles compared to wild type

plants, having an average value of  $139,82^{\circ}$ . In accordance with literature data the distribution of divergence angles was severely disturbed in the case of the *blr* line.

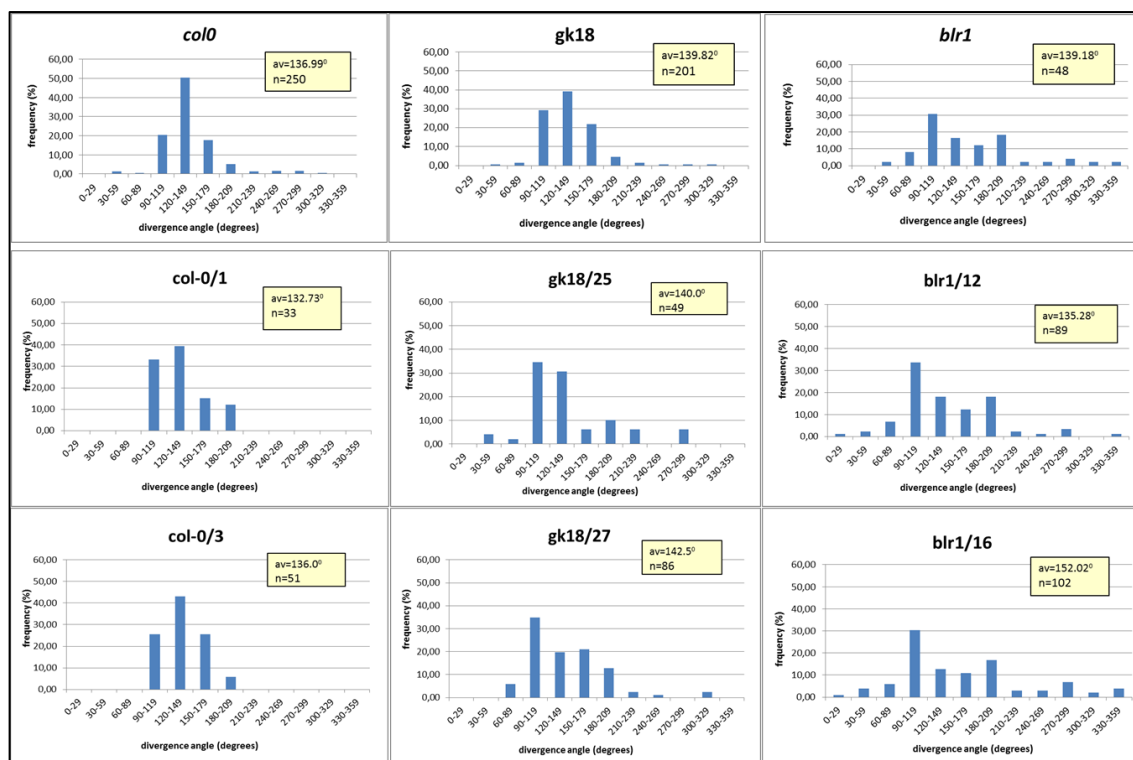


Figure 9. Main inflorescence phyllotaxy of *col0*, *rlck\_via2* (*gk18*) and *blr1* knock out lines (first row) and of T1 plant generation of *rlck\_via2 OX* in *col0*, *rlck\_via2 CO* in *gk18* and *rlck\_via2 OX* in *blr1* transformed lines (second and third row). Divergence angles between two successive siliques on the stem were allocated into twelve  $30^{\circ}$  classes and the percentage of total measurements ( $n$ ) falling into each is displayed. The average angles (av) are also presented.

In the case of the overexpressor lines *rlck\_via2 OX* in *col0* (*col-0/1*, *col-0/3*) and *rlck\_via2 OX* in *blr* (*blr/12* and *blr/16*) the expression of RLCK\_VI\_A<sub>2</sub> under the control of the strong CaMV 35S promoter slightly flattened the Gaussian distribution of divergence angles by broadening their range and increasing their frequency. Its effect was more pronounced in the complementing lines *rlck\_via2 CO* in *gk18* (*gk18/25* and *gk18/27*), where a more severe phyllotactic disturbance could be detected at the level of both range and frequency of divergence angles. The ectopic expression of the kinase in these lines could not complement the slight phyllotactic disturbance observed in the kinase knock out line *gk18* (Fig. 9., second column). The negative effect of the ectopic kinase expression was accentuated in the T2 generation plants of the transformed lines, where the disruption of “wild-type” phyllotaxy could be detected in all three lines discussed above (Fig. 10.)

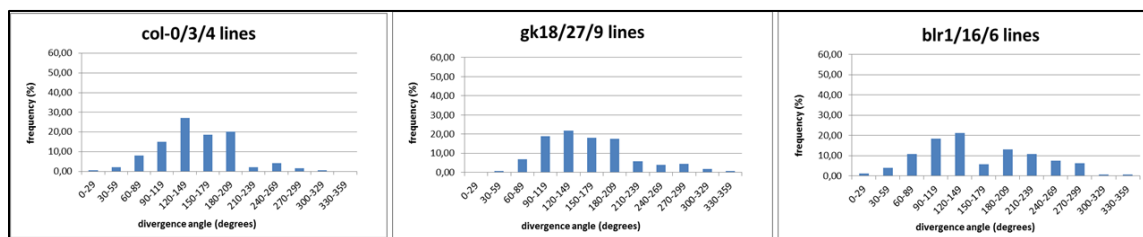


Figure 10. Altered phyllotaxis in the main inflorescence stem meristem of the T2. plant generation of *rlck\_via2 OX* in *col0*, *rlck\_via2 CO* in *gk18* and *rlck\_via2 OX* in *blr* lines.

Internode lengths between two successive fruits were also determined on images taken from stems with the aim of ImageJ software. Data were displayed as distribution of internode length between two successive siliques along the stem. The percentage of total internode lengths (frequency %) falling into each of eleven classes of 3 mm are shown (Fig11.). Wild type *col0* presented a Gaussian-like distribution curve of internode lengths peaking at 6÷9 mm correlating with literature data (Peaucelle *et al.*, 2011b). The *blr* line showed the most frequent internode length at 0÷3 mm, meaning that in this mutant silique are often placed very close to each other on the stem (Fig7., red arrows). Similar phenotype was described by Peaucelle A *et al.* for the *blr6* mutant (Peaucelle *et al.*, 2011b). The kinase knock-out mutant *gk18*, has siliques slightly closer to each other since the frequency of the 0÷3 mm internode distance is doubled compared to *col0* (Fig11.). As in the case of radial phyllotaxy, the ectopic expression of RLCK\_VIA<sub>2</sub> kinase disturbed the frequency of internode distances in all genetic backgrounds.

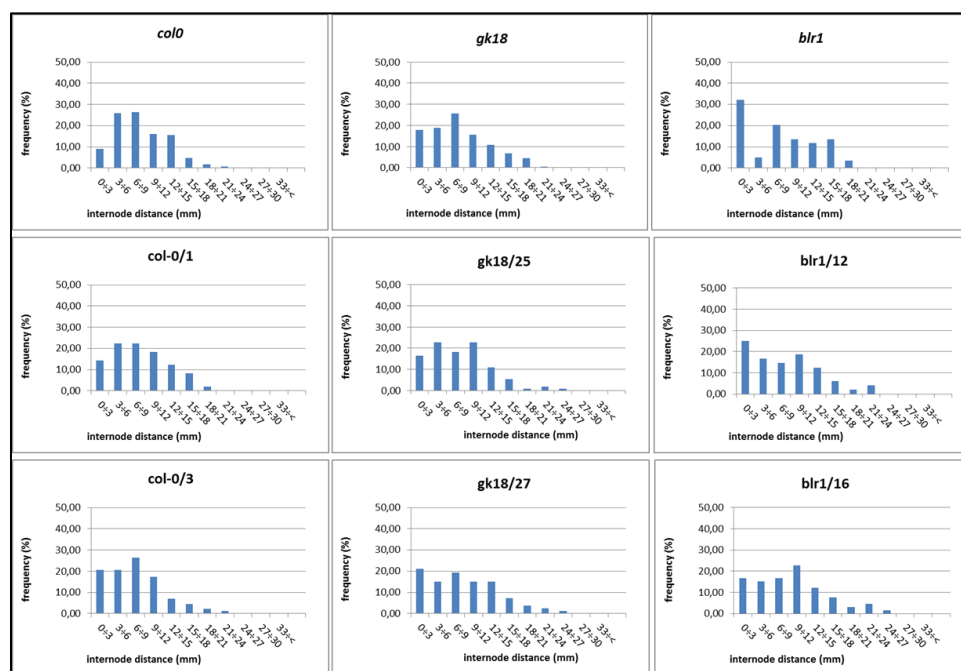


Figure 11. Internode length in *col0*, *rlck\_via2 (gk18)* and *blr* knock out lines (first row) and in T1 plant generation of *rlck\_via2 OX* in *col0*, *rlck\_via2 CO* in *gk18* and *rlck\_via2 OX* in *blr* transformed plant lines (second and third row).

**Investigation of Arabidopsis replums.** There are number of reports regarding the involvement of BELLRINGER in *Arabidopsis thaliana* (*At*) fruit development. The *At* fruit wall consists of three principal tissues: the valves (or seedpod walls), the replum (or central ridge between valves) and the valve margins, where the valves separate from the replum to disperse the seeds. The replum was classically defined as the structure that remains attached to the plant after the valves have fallen from the fruit at maturity and includes the septum (Weberling, 1992). Recently the replum is defined as the outer region that does not include the internal septum (Alvarez and Smyth, 2002).

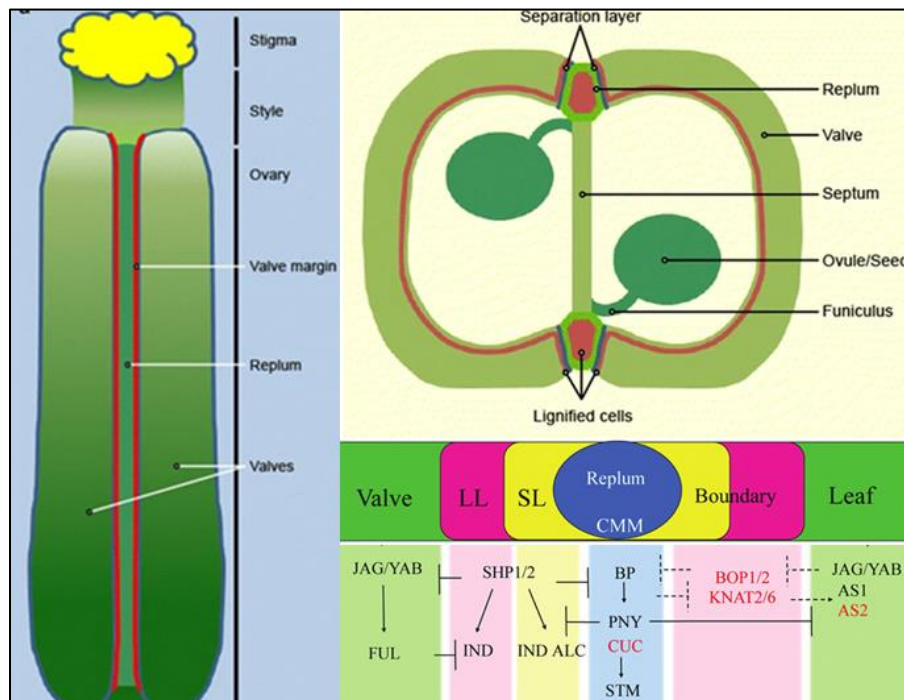


Figure 12. Schematic of an Arabidopsis fruit and summary of networks involved in fruit patterning and in the definition of the SAM-leaf boundary.

LL-lignified layer, SL-separation layer, CMM-carpel marginal meristem, BP-BREVIPEDICELLUS, PNY-BELLRINGER PENNYWISE, CUC-CUP SHAPED COTYLEDON, STM-SHOOT MERISTEMLESS, SHP1/2-SHATTERPROOF 1/2, BOP1/2-BLADE ON PETIOLE 1/2, KNAT2/6-KNOTTED IN ARABIDOPSIS THALIANA2/6, IND-INDEHISCENT, ALC-ALCATRAZ, FUL-FRUITFULL, JAG/YAB-JAGGED/YABBY, AS1/2-ASYMMETRIC LEAVES 1/2. (Hepworth and Pautot, 2015; łangowski *et al.*, 2016).

According to several literature data (González-Reig *et al.*, 2012; Hepworth and Pautot, 2015; Łangowski *et al.*, 2016) the replum expresses meristematic genes (medial factors) that specify its development. One of those TFs is BELLRINGER (BLR), also called REPLUMLESS (or RPL). Its expression zone is the blue zone on Fig12., whereas the function of genes that work in leaves (lateral factors) determines the development of valves and valve margins – green, pink and yellow columns on Fig. 12. Consequently, the medial and the lateral pattern elements of the fruit apparently mimic the antagonistic relationships between the shoot meristem and the leaves. Medial factors such as BREVIPEDICELUS, BELLRINGER or CUP SHAPED COTYDELON autonomously constrain lateral factors so that they only express outside the replum, and lateral factors negatively regulate the medially expressed BP gene in a non-autonomous fashion to ensure correct replum development. As described earlier (Roeder *et al.*, 2003), the siliques of *blr* (or *rpl*) mutant plants had only a narrow structure composed of valve margin (vm) cells (Fig. 13.).

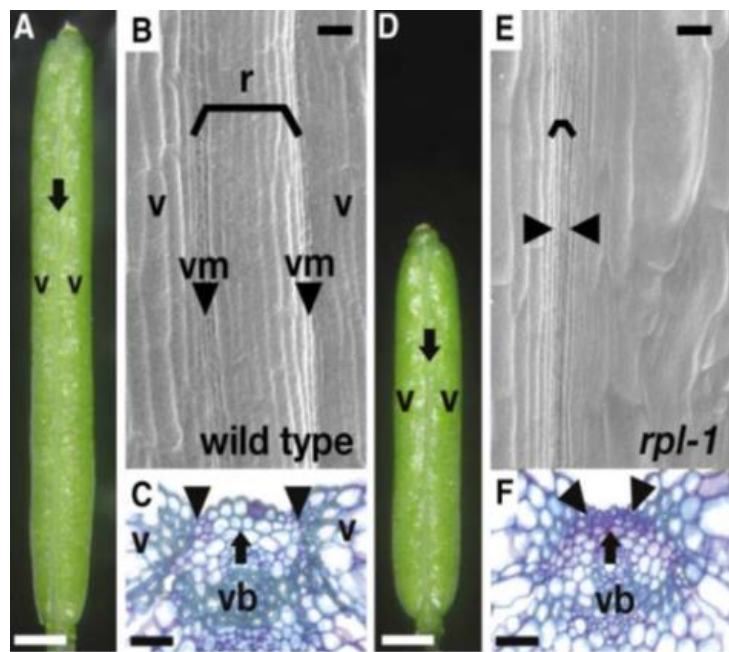


Figure 13. Structure of replum in wild type fruit and in the *rpl* mutant. The replum (r in B) is the ridge of cells between the valves (v in B and C). The valve margins (vm in B), where the valves join the replum, are composed of narrow cells (F). In the *rpl* fruit, the replum region (arrow in E) contains narrow cells that are like valve margin cells. Only the outer cell layers are affected and the inner vascular bundle (vb in C and F) is present (Roeder *et al.*, 2003).

It is supposed that the *BLR* gene is required to prevent the ectopic expression of valve margin markers in the replum. This is consistent with the appearance of valve margin-like cells in the replum region of *blr* (or *rpl*) mutants. With the aim of scanning electron microscopy, we investigated are there any differences in the structure of replums belonging to the above described and studied plant lines. Replums from mature, but young plants were collected and prepared for SEM, imaging was made with

the same zooming and same camera settings, so images taken at different times can be compared to each other. Wild type plants showed the widest replum, whereas *blr* replums were narrow in agreement to literature data. In the case of the kinase knock-out line (*gk18*) siliques had replums almost like wild type, some of them being slightly narrower, indicating that the absence of the kinase RLCK VI\_A<sub>2</sub> might have impact on replum formation (Fig. 14). Interestingly, a significant fraction of replums from this line presented less pronounced valve margins as wild type replums (Fig. 15).

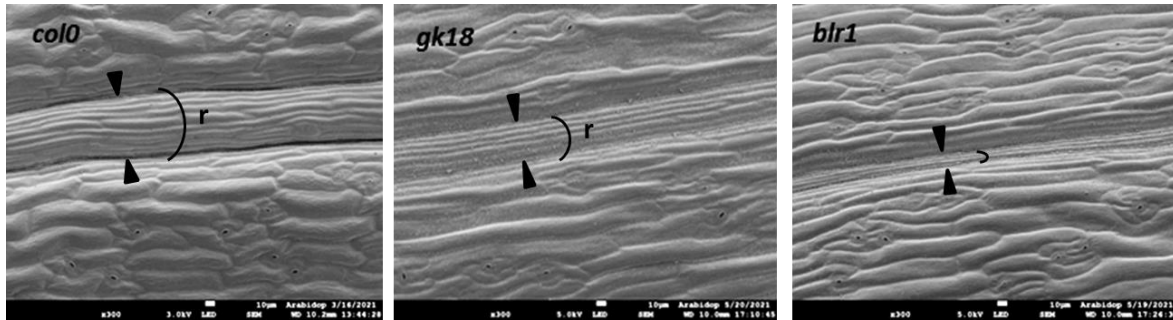


Figure 14. Representative SEM images of *Col0*, *rlck vi\_a2* KO (*gk18*) and *blr1* replums (r-replum, arrowheads-valve margins). Wild type columbia plants showed the wider replum, whereas *blr1* replums were narrow corresponding to literature data. In the case of the kinase knock-out line (*gk18*) siliques had replums almost similar to wild type, some of them being slightly narrower, indicating that the absence of the kinase VI\_A<sub>2</sub> might have impact on replum formation.

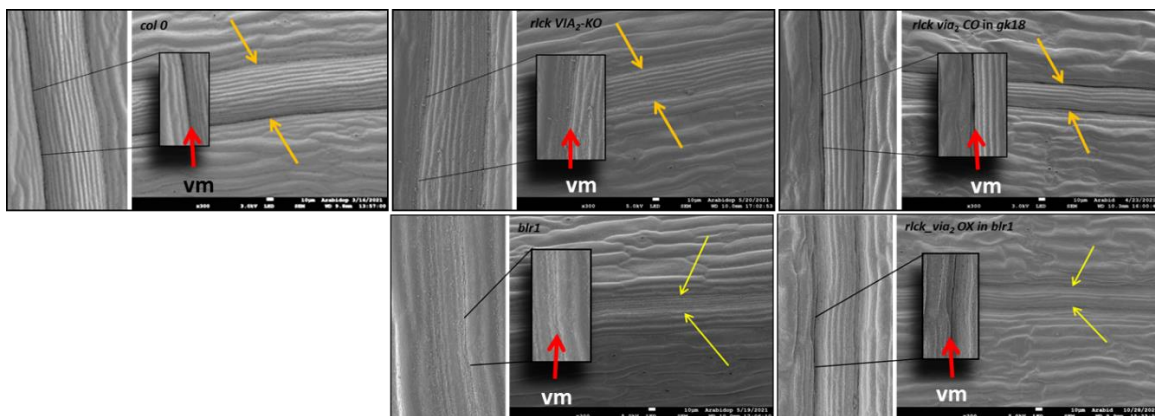


Figure 15. Representative SEM images of *col0*, *rlck vi\_a2* KO (*gk18*) and *rlck vi\_a2* CO in *gk18* replums (upper row) and of *blr1* and *rlck vi\_a2* OX in *blr1* (lower row). Yellow arrows indicate the replum, vm and red arrows indicate the valve margin. A significant fraction of replums from the *gk18* line presented less pronounced valve margins as wild type replums. When the *gk18* line was complemented with the RLCK VI A<sub>2</sub> kinase showing ectopic expression (in the *rlck vi\_a2* CO in *gk18* line) replums became slightly narrower, but the structure of the boundary between valve and replum (valve margins) was restored and in some cases became deeper compared with wild type *col-0*. The ectopic expression of RLCK VI\_A<sub>2</sub> could restore the structure of replums in the case of the transformed *blr-1* line also as indicated by images of the lower row.

When the *gk18* line was complemented with the ectopically expressed kinase gene (in the *rlck vi\_a2* *CO* in *gk18*) replums became even narrower, but the structure of the boundary between valve and replum was restored or in some cases was more pronounced (deeper), than *col-0* replums (Fig. 15). The ectopic expression of RLCK VI\_A<sub>2</sub> could restore the structure of replums in the case of the transformed *blr* line also (Fig. 15).

Studies of replum structure and fruit development showed that wild-type valve margin consists of a lignified layer and a separation layer; it was also shown that in the *blr* mutant replum cells are changed by separation layer cells (Roeder *et al.*, 2003). It seems that the ectopic expression of RLCK VI\_A<sub>2</sub> is able to restore the initial structure of replum. To verify this hypothesis and also to detect the modifications appeared at tissue level; cross-sections of replum regions were done and stained with toluidine-blue and phloroglucinol. This investigation is still going on, but preliminary studies showed us that the ectopic presence of the kinase might interfere with the morphology of tissues present in replum.

**In summary: the BLR transcription factor is important for the regulation of RLCK VI\_A<sub>2</sub> expression – in *blr* mutants the expression of the *rlck vi\_a2* gene is barely detected. The ectopic expression of *rlck vi\_a2* gene could not complement the phyllotactic phenotype of the *blr* mutation but rather strengthened it. The ectopic expression of the kinase interfered with normal phyllotaxis even in the presence of BLR in wild-type and kinase mutant genetic backgrounds. It indicates that the kinase negatively controls phyllotaxis if expressed from a constitutive promoter out of the control of BLR. In contrast, the ectopic expression of RLCK VI\_A<sub>2</sub> kinase could restore the structure of replums in the *blr* line. These observations highlight the significance of the spatial control of RLCK VI\_A<sub>2</sub> expression by BLR.**

**Publication in preparation:**

**Beöthy-Fehér O, Kenesi E, Valkai I, Domonkos I, Szóllósy R, Fehér A.** The REPLUMLESS transcription factor controls the expression of the ROP-activated RLCK VI\_A<sub>2</sub> kinase being involved in meristem functions.

**Hypothesis 3. ROP signalling modules influence organ development via auxin distribution.**

We first approached this hypothesis studying the function of the ROP-activated kinase RLCK VI\_A<sub>2</sub> during seedling establishment and plant growth. For this purpose, loss-of-function lines (T-DNA insertion, RNA-interference-mediated silencing) were identified/produced and analyzed. The analyses

indicated that the kinase function is rather required for cell elongation and not for meristem functioning. Furthermore, among the plant hormones only exogenous gibberellic acid (GA) known as one of the key regulators of plant cell elongation could complement the phenotypes (short hypocotyl, small leaves) caused by the loss of kinase function. Interestingly, however, we could not detect change neither in the GA level, nor in GA signaling in the mutant in comparison to the wild type. Transcriptome analysis showed that indeed gibberellin is not a likely direct target of the kinase. Its absence rather affected the metabolism and signaling of other hormones, such as auxin. Furthermore, the transcriptomic changes revealed that the loss of RLCK VI\_A2 alters cellular processes related to cell membranes, cell periphery, and apoplast. These processes are involved in cellular transport and/or cell wall reorganization. It was hypothesized, therefore that gibberellins and the RLCK VI\_A2 kinase work in parallel to promote cell expansion and plant growth. Gene expression studies also suggested that the kinase may have a role in controlling hypocotyl/cotyledon elongation overlapping with the action of the transcription factor circuit (PIF4-BZR1-ARF6) integrating various hormonal (including GA) and environmental signals to control hypocotyl elongation (and plant growth). Since these results have been published in the open access International Journal of Molecular Sciences (IF: 5.924 (2020)) including the detailed transcriptomic analysis of the mutant, we do not discuss here the details. The published paper is available via the following link: <https://doi.org/10.3390/ijms21197266>.

To identify the signaling pathways the ROP GTPase-activated RLCK VI\_A2 kinase is potentially involved, we used various proteomic approaches. The 3xMYC-tagged RLCK VI\_A2 kinase was expressed in transgenic plants and the kinase was immunoprecipitated by anti-MYC antibody coated beads. The co-immunoprecipitated proteins were identified by MALDI sequencing. Unfortunately, despite repeated trials, the approach failed. Even the bait kinase protein could hardly be detected in the immunoprecipitated, and further proteins were only represented by very limited number of peptides (Fig. 16). These results agreed with other observations that the expression level of the kinase is rather uncertain even if controlled by a constitutive promoter (see above). In summary, no significant conclusions could be drawn from the experiments. Pre-selection of a line with high expression could be a solution, although that may more likely convey artificial results. Furthermore, the kinase-substrate interactions are likely too transient and weak to be detected in this way. Therefore, we constructed vectors carrying the kinase cDNA fused to the sequence of the TurboID tag allowing the application of proximity biotiny

Fuson /UP2017_ARA_spall_realUP 54820				180404_03_FA_VI_cmyc/up2017ara 12731									
Rank	Acc #	Gene	Num U	Peptide	unt	% Cov	Num U	Peptide	unt	% Cov	Protein MW	Species	Protein Name
[361]	O64619	At2g18890	1,82E-06	8	9	0,000707	25	44533,6	ARATH	At2g18890	44533,6	ARATH	At2g18890
[499]	Q9LJG3	ESM1	1,82E-06	5	6	0,000471	21,2	44060,7	ARATH	GDSL esterase/lipase ESM1	44060,7	ARATH	GDSL esterase/lipase ESM1
[799]	Q9M8D3	At1g74260	1,82E-06	5	5	0,000393	5,8	153955	ARATH	Probable phosphoribosylformylglycinamide synthase, chloroplasti	153955	ARATH	Probable phosphoribosylformylglycinamide synthase, chloroplasti
[801]	Q5XF82	JAL11	1,82E-06	5	5	0,000393	14,4	48524,1	ARATH	Jacalin-related lectin 11	48524,1	ARATH	Jacalin-related lectin 11
[709]	Q9SU40	SKU5	1,82E-06	4	4	0,000314	10,1	65638,3	ARATH	Monocopper oxidase-like protein SKU5	65638,3	ARATH	Monocopper oxidase-like protein SKU5
[822]	Q5XF32		1,82E-06	4	4	0,000314	13,4	44162,3	ARATH	3-isopropylmalate dehydrogenase	44162,3	ARATH	3-isopropylmalate dehydrogenase
[827]	Q0WL29	At5g24710	1,82E-06	4	4	0,000314	4,8	126036,3	ARATH	Uncharacterized protein At5g24710	126036,3	ARATH	Uncharacterized protein At5g24710
[940]	Q0WPF4	At3g45300	1,82E-06	4	4	0,000314	15,9	44773,6	ARATH	Isovaleryl-CoA-dehydrogenase	44773,6	ARATH	Isovaleryl-CoA-dehydrogenase
[974]	Q2LHB9	PER32	1,82E-06	4	4	0,000314	13,4	38847,4	ARATH	Peroxidase 32	38847,4	ARATH	Peroxidase 32
[1993]	Q9SXA1	PI4KA1	1,82E-06	3	4	0,000314	2,4	224018,9	ARATH	Phosphatidylinositol 4-kinase alpha 1	224018,9	ARATH	Phosphatidylinositol 4-kinase alpha 1
[886]	Q0WMT9	ALDH6B2	1,82E-06	3	3	0,000236	8,4	65927,1	ARATH	Methylmalonate-semialdehyde dehydrogenase [acylating], mitochond	65927,1	ARATH	Methylmalonate-semialdehyde dehydrogenase [acylating], mitochond
[906]	Q50039	OTC	1,82E-06	3	3	0,000236	14,4	41002,4	ARATH	Ornithine carbamoyltransferase, chloroplasti	41002,4	ARATH	Ornithine carbamoyltransferase, chloroplasti
[927]	Q94BR2	AILP1	1,82E-06	3	3	0,000236	22,2	25015,5	ARATH	Aluminum induced protein with YGL and LRDR motifs	25015,5	ARATH	Aluminum induced protein with YGL and LRDR motifs
[944]	O48661	SPDSYN2	1,82E-06	3	3	0,000236	12,4	37140,5	ARATH	Spermidine synthase 2	37140,5	ARATH	Spermidine synthase 2
[1067]	Q8LBG6		1,82E-06	3	3	0,000236	12,6	34962,4	ARATH	Putative NADPH dependent mannose 6-phosphate reductase	34962,4	ARATH	Putative NADPH dependent mannose 6-phosphate reductase
[1073]	Q9SQT8	EMB3004	1,82E-06	3	3	0,000236	6,8	65796,7	ARATH	Bifunctional 3-dehydroquinate dehydratase/shikimate dehydrogenase	65796,7	ARATH	Bifunctional 3-dehydroquinate dehydratase/shikimate dehydrogenase
[1087]	O22940	At2g41800	1,82E-06	3	3	0,000236	11,1	40370,8	ARATH	At2g41800/T11A7.10	40370,8	ARATH	At2g41800/T11A7.10
[1108]	O22842	At2g43610	1,82E-06	2	3	0,000236	11,4	29999,8	ARATH	Endochitinase At2g43610	29999,8	ARATH	Endochitinase At2g43610
[1133]	Q92VU4	At1g55450	1,82E-06	3	3	0,000236	13,8	34475,7	ARATH	At1g55450/T5A14.14	34475,7	ARATH	At1g55450/T5A14.14
[1169]	Q93Y08	ABC1K8	1,82E-06	3	3	0,000236	4,5	86024,1	ARATH	Protein ACTIVITY OF BC1 COMPLEX KINASE 8, chloroplasti	86024,1	ARATH	Protein ACTIVITY OF BC1 COMPLEX KINASE 8, chloroplasti
[1174]	Q9SSB7	DGR1	1,82E-06	3	3	0,000236	13,8	40226,6	ARATH	At1g80240	40226,6	ARATH	At1g80240
[1283]	Q945N7		1,82E-06	3	3	0,000236	8,9	56717,9	ARATH	AT5g04420/T32M21_20	56717,9	ARATH	AT5g04420/T32M21_20
[1661]	Q8LPK4	ALPHAC-AD	1,82E-06	3	3	0,000236	7,2	112299,9	ARATH	AP-2 complex subunit alpha-2	112299,9	ARATH	AP-2 complex subunit alpha-2
[1769]	Q8L606	At3g53560	1,82E-06	3	3	0,000236	9,1	38664,9	ARATH	Tetratricopeptide repeat (TPR)-like superfamily protein	38664,9	ARATH	Tetratricopeptide repeat (TPR)-like superfamily protein

Figure 16. List of the first 30 proteins co-immunoprecipitated with the RLCK VI\_A2 kinase (At2G18890). The green columns show the number of peptides representing the given proteins. Result of the best experiment (with more own peptides of the kinase) is shown as example.

labeling of even temporarily kinase associated proteins (Kim *et al.*, 2019). Construction was made with cDNAs coding for wild-type and kinase-dead mutant RLCK VI\_A2. The constructs have already been tested in transient expression experiments. Interestingly while strong expression of the kinase-dead protein could be achieved, the parallel experiments with the wild type kinase resulted in hardly detectable protein expression. These results again indicated that the kinase might negatively control its own stability/level in plant cells. We are currently working to overcome this problem.

In a parallel approach, we initiated a collaboration with the University of Warwick (Jose Gutierrez-Marcos, Julius Durr; (Durr *et al.*, 2021)) to carry out phosphoproteomic experiments with the aim of identifying potential RLCK VI\_A2 substrates. The phosphoproteome of wild-type and RLCK VI\_A2 mutant seedlings was compared in three repetitions. Altogether 837 differentially phosphorylated proteins could be identified as statistically significant and represented by at least three different peptides in the samples. Surprisingly, only 18 of them exhibited lower phosphorylation rate in the kinase mutant than in the control, all the other were represented by significantly more phosphorylated peptides in the wild-type than in the mutant. It is contrast with the expectations for the effect of a kinase mutation (Figure 15). One can suppose that these phosphorylations are indirect consequences of the loss-of RLCK VI\_A2 function. Our hypothesis is, that RLCK VI\_A2-phosphorylated proteins might be destined for degradation. Thus, in the absence of the kinase they are more abundant and due to phosphorylation by other kinases are represented with more phosphorylated peptides in the mutant. This hypothesis is supported by the NPL4 protein that is underphosphorylated in the mutant in comparison to the wild type being involved in protein degradation on the proteasomal ubiquitin-dependent pathway (Fig. 17). We have already attempted to verify this hypothesis studying overall protein ubiquitination in the wild type and the kinase mutant; however, this approach was not

sensitive enough to highlight subtle differences caused by only a limited number of proteins. Therefore, potential candidates were selected for detailed analysis. First, we selected the BRAHMA chromatin modelling ATPase for further studies for various reasons: it was significantly more phosphorylated in the kinase mutant than in the wild type (Fig. 18); this chromatin remodeling protein plays roles in similar processes than the RLCK VI\_A2 kinase (BELLRINGER regulated phyllotaxis (Zhao *et al.*, 2015); GA and PIF4-regulated hypocotyl elongation without affecting GA level/signaling (Archacki *et al.*, 2013; Jégu *et al.*, 2017, page 60); flower organ boundaries (Sun and Ito, 2015); root meristem maintenance (Yang *et al.*, 2015). Moreover, the *brm-1* and the *rlck vi\_a2* mutants share 639 differentially expressed genes in comparison each to the wild type (data not shown). And last, in a yeast 2-hybrid screen, the RLCK VI\_A2 bait fished out the BRAHMA protein as a prey (see further for more details), indicating their potential in planta interaction.

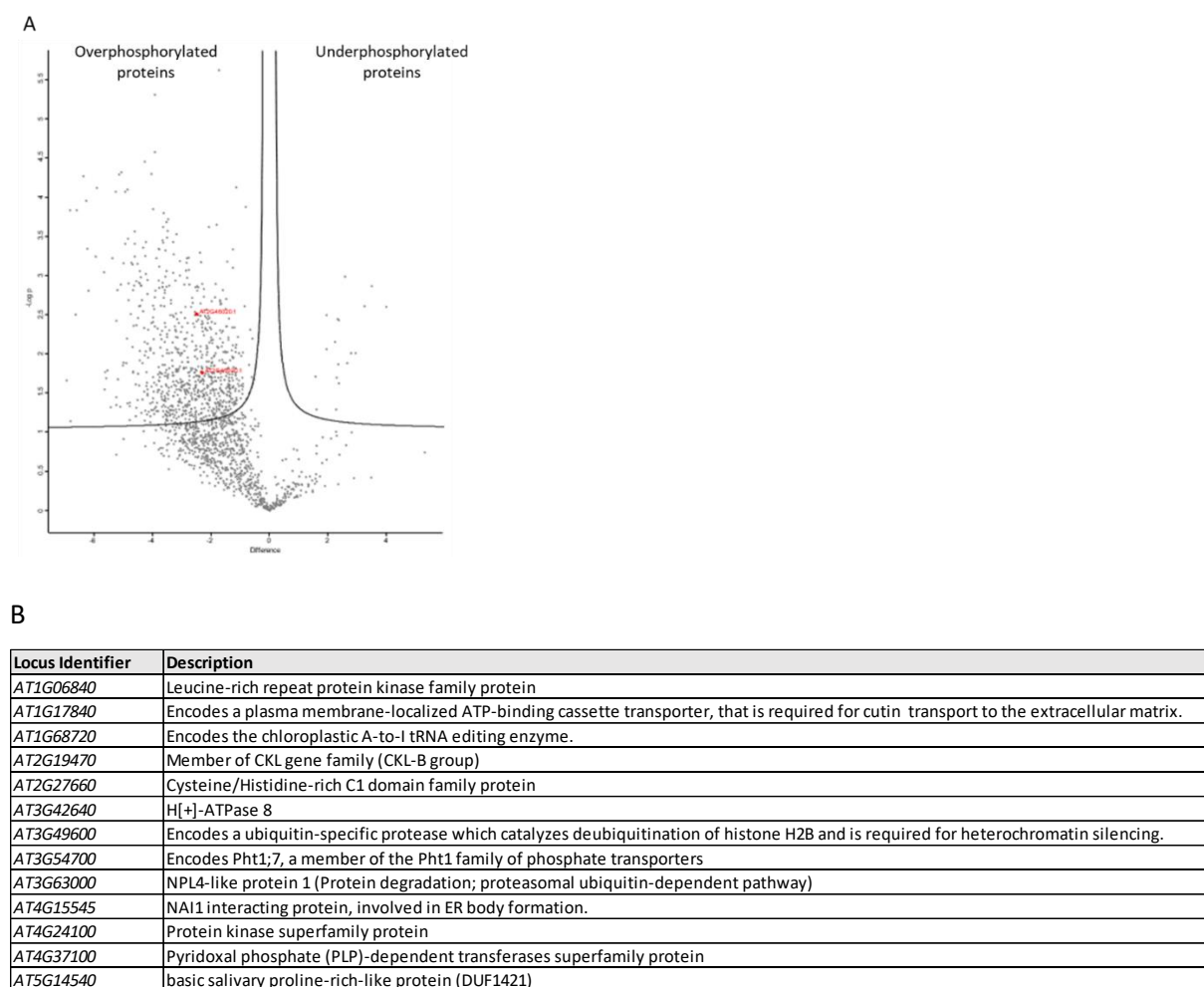


Figure 17. A) Histogram showing the distribution of over- or underphosphorylated proteins in kinase mutant seedlings in comparison to the wild type. B) The 13 proteins with decreased phosphorylation in the kinase mutant in comparison to the wild type (designated as “underphosphorylated” on part A).

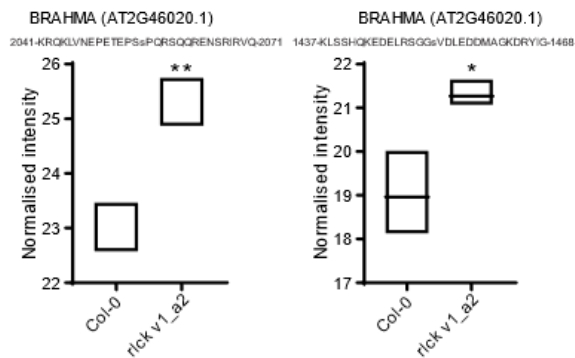


Figure 18. Representation of the BRAHMA protein by two phosphopeptides present in significantly higher quantity in the rick vi\_a2 kinase mutant than in the wild type (Col-0).

The yeast 2-hybrid screening of an Arabidopsis seedling library with the RLCK VI\_A2 kinase as a bait resulted in 342 sequenced clones. Sequence analysis revealed that the clones represent 169 different proteins. Based on their annotations, some of the kinase-interacting proteins could be classified into functional groups (Fig. 19). They were also classified according to their interaction strength with the kinase in yeast (data not shown).

One of the interactors was the Rop11 GTPase in agreement with the fact that the kinase is RopGTPase activated (DORJGOTOV *et al.*, 2009). This is further strengthened by our experiments proving that 85 out of the 169 clones interacting with RLCK VI\_A2 also interacted with ROP11.

#### Transcription factors (30)

12 SANT/MYB TF  
12 Homeobox-like domain TF

#### Chromatin remodelling factors

AT4G02020 SET domain-containing protein;  
AT1G63490 transcription factor jumonji (jmjC) domain-containing protein  
AT2G46020 transcription regulatory protein SNF2; BRAHMA  
AT5G09790 TRITHORAX-RELATED PROTEIN 5;

#### RNA-binding/exosome

AT1G59760 RNA helicase, ATP-dependent, SK12/DOB1 protein;  
AT1G73490 RNA-binding (RRM/RBD/RNP motifs) family protein;  
AT3G56510 RNA-binding (RRM/RBD/RNP motifs) family protein;  
AT4G26000 RNA-binding KH domain-containing protein;  
AT1G21580 Zinc finger C-x8-C-x5-C-x3-H type family protein;

#### Protein ubiquitination

AT1G08315 ARM repeat superfamily protein;  
AT2G26780 ARM repeat superfamily protein;  
AT4G12710 ARM repeat superfamily protein;  
AT4G38120 ARM repeat superfamily protein;  
AT5G65920 ARM repeat superfamily protein;  
AT2G46260 BTB/POZ/Kelch-associated protein;  
AT1G08710 F-box family protein;  
AT2G35930 plant U-box 23;  
AT1G73760 RING/U-box superfamily protein;  
AT2G40640 RING/U-box superfamily protein;  
AT3G29160 SNF1 kinase homolog 11;  
AT1G63800 ubiquitin-conjugating enzyme 5;  
AT5G65450 ubiquitin-specific protease 17;

#### Vesicular transport

AT1G56590 Clathrin adaptor complexes medium subunit family protein;  
AT2G21190 ER lumen protein retaining receptor family protein;  
AT5G57460 muniscin carboxy-terminal mu-like domain protein;  
AT5G64070 phosphatidylinositol 4-OH kinase beta1;  
AT2G43130 P-loop containing nucleoside triphosphate hydrolases superfamily protein;  
AT2G35210 root and pollen arfgap;  
AT3G45280 syntaxin of plants 72;

Figure 19. Classification of some of the RLCK VI\_A2-interacting proteins (based on yeast 2-hybrid screening results). Note the high numbers of transcription factors and chromatin remodellers (30+4) and proteins implicated in protein degradation (13).

BRAHMA (At2G46020 SET domain-containing protein) was one of the two proteins that were highlighted both in the phosphoproteomic and yeast-2-hybrid approaches as potential RLCK VI\_A2 targets (the other one was a nuclear protein involved in RNA quality control). The BRAHMA protein is huge: 245 kD. Therefore, in parallel to clone the full sequence (6578 bp) we started to work with the C-terminal fragment obtained by the 2-hybrid screening as interacting with the kinase. The purified BRAHMA fragment could be phosphorylated by the purified kinase (Fig. 20A). The effect of the kinase on in planta BRAHMA stability was tested in Arabidopsis seedlings transfected with a plasmid construct expressing MYC-tagged RLCK VI\_A2 and HA-tagged BRAHMA fragment. As negative controls, a construct expressing a kinase-dead RLCK VI\_A2 (YA; (Lajkó *et al.*, 2018)) together with BRAHMAfr, and two other constructs expressing HA-tagged YELLOW FLUORESCENT PROTEIN (YFP) instead of BRAHMA together with the kinase variants were used. While the BRAHMA fragment could not

be detected in the presence of the active kinase but was detectable if the kinase dead mutant was expressed, the presence of the YFP protein was independent of the kinase variants. Therefore, one can suppose that the kinase affected the instability of the BRAHMA fragment (Fig. 20B).

These results have been presented at two conferences as lectures: **Plant Biology Europe 2021** (Turin, Italy) 28.06-01-07. 2021 [https://euoplantbiology2020.org/wp-content/uploads/2021/06/PBE2021-final-program\\_29.06.21.pdf](https://euoplantbiology2020.org/wp-content/uploads/2021/06/PBE2021-final-program_29.06.21.pdf)); **XIII. Magyar Növénybiológiai Kongresszus**, Szeged, 2021. augusztus 24-27.).

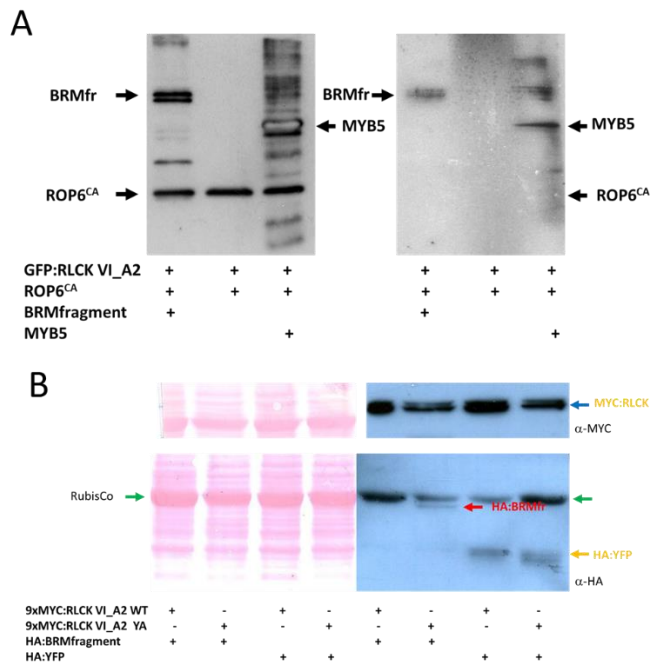


Figure 20. A) In vitro kinase assay showing the presence of the 6xHIS-tagged proteins in the kinase assay mixtures as indicated (left immunoblot) and the phosphorylated protein fraction of the same assays using anti-phosphoserine/threonine antibody (right immunoblot). B) Detecting the MYC-tagged kinase and the HA-tagged BRAHMA fragment or YFP protein co-expressed in Arabidopsis seedlings in the indicated combinations. Note that the anti-HA antibody also labelled the abundant RubisCO protein.

**In summary: Investigating the biological functions of the RLCK VI\_A2 ROP-activated kinase using mutant analysis, transcriptomics, phosphoproteomics and yeast 2-hybrid screening revealed its role in cell/organ elongation/growth likely via interfering with proteosomal protein degradation and/or gene expression regulation rather than directly regulating auxin transport. The rlc vi\_a2 mutation affected gene expression pathways point to the role of the kinase in extracellular/apoplastic processes. Several potential protein targets of the kinase were identified. Ongoing studies aim to provide further evidence to confirm the biological significance of these interactions to strengthen the scientific impact of the findings.**

#### Publications:

**Valkai I, Kénesi E, Domonkos I, Ayaydin F, Tarkowská D, Strnad M, Faragó A, Bodai L, Fehér A.** 2020. The Arabidopsis RLCK VI\_A2 Kinase Controls Seedling and Plant Growth in Parallel with Gibberellin. *International Journal of Molecular Sciences* 21, 7266. (IF: 5.924 (2020))

#### Invited conference lectures:

**Ildikó Valkai, Dézi B. Lajkó, Erzsébet Kenesi, Dalma Ménesi, Péter Borbély, László Bodai, Julius Durr, Attila Fehér** ROP GTPase-activated kinase signaling in Arabidopsis **Plant Biology Europe 2021** (Turin, Italy) 28.06-01-07.

**Fehér A, Valkai I, Lajkó DB, Kenesi B, Ménesi D, Borbély P, Bodai L, Julius Durr.** ROP GTPáz aktivált kináz jelátvitel növényekben. **XIII. Magyar Növénybiológiai Kongresszus**, Szeged, 2021. augusztus 24-27.

**Hypothesis 4:** ROP7/ROP3 signaling module linked to unknown upstream/downstream kinases regulates root meristem maintenance.

Unfortunately, we faced several technical difficulties also already during the initial efforts to validate this hypothesis such as non-specific commercial ROP3/RopGEF7 antibodies, RopGEF7 gene expression in *ropgef7* mutant seeds obtained from a seed bank. Although we could see *in vitro* phosphorylation of RopGEF7 by calcium-dependent kinases (CPKs) and the CPK-related kinase CRK5, we could not unambiguously determine the phosphorylation sites which were any way many (data not shown). This prevented our original phospho-site mutagenesis approach. Furthermore, the gene expression analysis of the *r1ck vi\_a2* mutant and wild type *Arabidopsis* roots identified 561 statistically significant DEGs (differentially expressed genes). GO annotation could not reveal significant enrichment of the DEGs except those associated with stress responses (data not shown).

However, during the *in vitro* phosphorylation approaches it was revealed that CPKs can also phosphorylate the ROP GTPase. Since we have published earlier the potential significance of ROP GTPase phosphorylation in the regulation of its interaction with RopGEFs (Fodor-Dunai *et al.*, 2011), we carried out experiments to investigate whether the ROPs are phosphorylated by CPKs at the amino acid motif affecting RopGEF binding. The experiments, however, revealed that CPKs can *in vitro* phosphorylate the ROPs at other motifs and the biological significance of this phosphorylation remained obscure despite our attempts to investigate its interference with protein interactions and functions of the phosphomimic ROP1 mutants. The details of the approach and the results are published in a paper in *Plants* (IF: 4.658 (2021)) accessible at <https://doi.org/10.3390/plants10102053>.

Furthermore, since we had plant lines carrying mutation in the CRK5 gene expressing auxin and auxin transport marker genes, we investigated its involvement in root meristem maintenance, embryogenesis, and seedling establishment. This collaborative research with Dr. Gábor Rigó (BRC, Szeged) resulted in three open access publications in the *International Journal of Molecular Sciences* two in 2019 (IF: 4.556) and one in 2021 (IF: 6.208), respectively. These publications can be accessed at <https://doi.org/10.3390/ijms20246120>; <https://doi.org/10.3390/ijms20143432>; <https://www.mdpi.com/1422-0067/22/11/5979>. Therefore, here we summarize only the main findings:

1. We showed that the embryogenesis of the *Atcrk5-1* mutant is delayed in comparison to the wild type. This delay is accompanied with a decrease in the levels of GA and auxin, as well as the abundance of the polar auxin transport (PAT) proteins PIN1, PIN4, and PIN7 in the mutant embryos. Furthermore, it was demonstrated that CRK5 can phosphorylate the hydrophilic loop of various PIN proteins.
2. We described that the *Arabidopsis thaliana* CRK5 protein kinase influences auxin transport and the auxin-ethylene-GA hormonal crosstalk during hypocotyl hook formation/opening.
3. We proved the potential involvement of the CRK5 protein kinase in the coordination of the auxin-reactive oxygen species-nitric oxide-PIN2-auxin regulatory loop in the root meristem affecting the gravitropic response.

During the experiments it was observed that the *rop2-1* mutant responded differently to exogenous nitric oxide than the wild type: the root shortening effect of NO could not be observed in the absence of ROP2. NO was shown to inhibit primary root growth by altering the abundance and distribution of the PIN1 auxin efflux carrier protein and lowering the accumulation of auxin in the root meristem.

However, in *rop2-1* insertion mutant, wild type-like root size and wild type-like PIN1 abundance in the meristem of NO-treated roots were maintained. Furthermore, the ROP2 GTPase was shown to be S-nitrosylated *in vitro* suggesting that NO might directly regulate the GTPase. Based on this we prepared a manuscript claiming that the Arabidopsis ROP2 GTPase is a potential target of NO-mediated regulation of root meristem function. This manuscript was submitted to the Journal of Experimental Botany where it was rejected due to the missing *in planta* evidence of ROP nitrosylation. Since our efforts to provide the evidence failed (we could not immunoprecipitate sufficient amount of ROP2-promoter-driven GFP-tagged ROP2 from Arabidopsis seedlings), we decided to reorganise the manuscript and submit it to the journal Antioxidants (IF: 7.765 (2021)). I made accessible the manuscript at: <https://app.box.com/s/rcqxmvrhlx6rgxe118mew742m00z44>.

**In summary: although the hypothesis about the role of the potential CRK5-RopGEF7-Rop3 signalling pathway in root meristem functioning could not be proved, we revealed several details of root growth control affected by CRK5- and ROP GTPase-dependent signalling.**

#### Publications:

1. **Ménesi, D., Klement, É.,** Ferenc, G., and **Fehér, A.** (2021). The Arabidopsis Rho of Plants GTPase ROP1 Is a Potential Calcium-Dependent Protein Kinase (CDPK) Substrate. *Plants*. 10.3390/plants10102053.
2. **Cséplő, Á.,** Zsigmond, L., András, N., Baba, A.I., Labhane, N.M., Petkó-Szandtner, A., Kolbert, Z., Kovács, H.E., Steinbach, G., Szabados, L., **Fehér, A.,** Rigó, G. (2021). The AtCRK5 Protein Kinase Is Required to Maintain the ROS NO Balance Affecting the PIN2-Mediated Root Gravitropic Response in Arabidopsis. *International Journal of Molecular Sciences*. 10.3390/ijms22115979.
3. Baba, A.I., **Valkai, I.,** Labhane, N.M., Koczka, L., András, N., Klement, É., Darula, Z., Medzihradszky, K.F., Szabados, L., **Fehér, A.,** Rigó, G., **Cséplő, Á.** (2019). CRK5 Protein Kinase Contributes to the Progression of Embryogenesis of Arabidopsis thaliana. *International Journal of Molecular Sciences*. 10.3390/ijms20246120.
4. Baba, A.I., András, N., **Valkai, I.,** Gorcsa, T., Koczka, L., Darula, Z., Medzihradszky, K.F., Szabados, L., **Fehér, A.,** Rigó, G., **Cséplő, Á.** (2019). AtCRK5 Protein Kinase Exhibits a Regulatory Role in Hypocotyl Hook Development during Skotomorphogenesis. *International Journal of Molecular Sciences*. 10.3390/ijms20143432.
5. **Kénesi, E.,** Kolbert, Z., Kaszler, N., **Klement, É., Ménesi, D.,** Molnár, Á., **Valkai, I.,** Feigl, G., Rigo, G., **Cséplő, Á.,** Lindermayr, C., **Fehér, A.** (2022) S-nitrosation of the ROP2 GTPase is involved in nitric oxide (NO)-induced root shortening in Arabidopsis. *Antioxidants* (under review).

#### Invited conference lecture:

Zsuzsanna Kolbert, **Ágnes Cséplő, Erzsébet Kénesi, Dalma Ménesi, Éva Klement,** Árpád Molnár, Gábor Feigl, Christian Lindermayr, Gábor Rigo, **Attila Fehér** On the roles of NO in controlling auxin transport at the Arabidopsis root meristem. 8th Plant Nitric Oxide International Meeting (7th – 9th July, 2021) Szeged, Hungary - online.

### Overall summary:

We faced several problems when we attempted to validate the four working hypotheses laid down in the project application such as unexpected results, unsuitable antibodies, lost expertise of transgenic plant generation and crossing, unavailable radioactive isotopes for kinase assays, and the several interruptions of experiments due to the COVID situation etc. However, during the experimentation we made several interesting observations that worthened pursuing. Therefore, we modified our specific research goals, however, maintained our interest in the involvement of the investigated proteins in the regulation of plant growth and development. These efforts resulted in a diversified research activity involving various collaboration partners. In this way we had access to a range of up-to-date technologies (transcriptomics, proteomics and phosphoproteomics, scanning electron microscopy etc.) and valuable plant lines (e.g., the *crk5* mutant expressing fluorescent auxin transport markers). Some results reached publications in high impact open access journals while others still wait for further verifications to be ready for publication. In addition, the wealth of data obtained by the screening approaches can serve as the basis of future research directions.

### Cited literature

1. Alvarez, J., and Smyth, D.R. *CRABS CLAW* and *SPATULA* genes regulate growth and pattern formation during gynoecium development in *Arabidopsis thaliana*. *Int. J. Plant Sci.* **163**, 17-41 (2002).
2. Byrne, M.E., Groover, A.T., Fontana, J.R. & Martienssen, R. Phyllotactic pattern and stem cell fate are determined by the *Arabidopsis* homeobox gene *BELLRINGER*. *Development* **130**, 3941-3950 (2003).
3. Kanrar, S., Bhattacharya, M., Arthur, B., Courtier, J. & Smith, H. M. Regulatory networks that function to specify flower meristems require the function of homeobox genes *PENNYWISE* and *POUND-FOOLISH* in *Arabidopsis*. *Plant J.* **54**, 924-937 (2008).
4. Kanrar, S., Onguka, O. & Smith, H. M. *Arabidopsis* inflorescence architecture requires the activities of *KNOX-BELL* homeodomain heterodimers. *Planta* **224**, 1163-7113 (2006).
5. Peaucelle, A., Louvet, R., Johansen, J. N., Salsac, F., Morin, H., Fournet, F., Belcram, K., Gillet, F., Höfte, H., Laufs, P., Mouille, G. & Pelloux, J., The transcription factor *BELLRINGER* modulates phyllotaxis by regulating the expression of a pectin methylesterase in *Arabidopsis*. *Development* **138**, 4733-4741 (2011)
6. Roeder, A. H., Ferrandiz, C. & Yanofsky, M. F., The role of the *REPLUMLESS* homeodomain protein in patterning the *Arabidopsis* fruit. *Curr. Biol.* **13**, 1630-1635 (2003).
7. Roeder, A.H.K & Yanofsky, M. F, Fruit Development in *Arabidopsis*, *The Arabidopsis Book*. (American Society of Plant Biologists), (2006)
8. Ung, N & Smith, H. M., Regulation of shoot meristem integrity during *Arabidopsis* vegetative development. *Plant Signal Behav* **6**, 1250–1252 (2011)
9. Weberling, F., Morphology of flowers and inflorescences, *R. J. Pankhurst Trans.* (Cambridge Univ. Press, Cambridge). p. 341. (1989).
10. Rutjens B, Bao D, van Eck-Stouten E, Brand M, Smeekens S, Proveniers M., Shoot apical meristem function in *Arabidopsis* requires the combined activities of three *BEL1*-like homeodomain proteins, *The Plant Journal* **58**, 641–654, (2009)
11. Bartlett M.E., Thompson B., Meristem identity and phyllotaxis in inflorescence development, *Frontiers in Plant Science* **5**, (508) (2014)
12. Peaucelle A., Morin H., Traas J., Laufs P., Plants expressing a *miR164*-resistant *CUC2* gene reveal the importance of post-meristematic maintenance of phyllotaxy in *Arabidopsis*, *Development* **134**, 1045-1050 (2007)

13. Łangowski Ł., Stacey N., Ostergaard L., Diversification of fruit shape in the Brassicaceae family, *Plant Reproduction* **29**, 149–163, (2016)
14. Hepworth S.R. and Pautot V.A., Beyond the Divide: Boundaries for Patterning and Stem Cell Regulation in Plants, *Frontiers in Plant Science* **6**, 1052-1071, (2015)
15. Gonzales-Reig S., Ripoll J. J., Vera A., Yanofsky M.F., Martinez-Laborda A., Antagonistic Gene Activities Determine the Formation of Pattern Elements along the Mediolateral Axis of the Arabidopsis Fruit, *PLOS Genetics*, **8(11)**, (2012)